

## Research Article

# Effect of Different Size ZnO Particle Doping on Dielectric Properties of Polyethylene Composites

Yujia Cheng , Guang Yu , and Zhuohua Duan 

Mechanical and Electrical Engineering Institute, University of Electronic Science and Technology of China, Zhongshan Institute, Zhongshan 528400, China

Correspondence should be addressed to Guang Yu; [yuguang@hrbust.edu.cn](mailto:yuguang@hrbust.edu.cn)

Received 11 April 2019; Accepted 8 July 2019; Published 31 December 2019

Academic Editor: Zehra Durmus

Copyright © 2019 Yujia Cheng et al. This is an open access article distributed under the Creative Commons Attribution License, which permits unrestricted use, distribution, and reproduction in any medium, provided the original work is properly cited.

In this article, low density polyethylene was used as a matrix polymer. The ZnO particles with diameters of 30 nm and 1  $\mu\text{m}$  were used as inorganic filler. The nano-ZnO particles after surface modification would disperse in the matrix uniformly. The nano-, micro-, and micro-/nano-ZnO/LDPE were prepared by melt blending. During the experiment, the microstructures of different composites were characterized and discussed by SEM and DSC. Besides, the micro- and nano-ZnO/LDPE underwent a breakdown test, conductance test, and dielectric spectrum test. The microscopic experimental results showed that the ZnO particles dispersed uniformly in the LDPE matrix. The crystallinity of composites was higher than that of pure LDPE. Among them, the maximum crystallinity was 39.77% when the nano-ZnO particle size was 30 nm. It was 16.1% higher than pure LDPE. The macroscopic experimental results showed that the effect of micro- and nano-ZnO particle doping on breakdown properties of polymers was different. Among them, the breakdown field strength of nano-ZnO/LDPE was the highest at 138.0 kV/mm, which was 8.24% higher than that of pure LDPE. The micro-/nano-ZnO/LDPE took second place, which was still higher than pure LDPE. As the thickness of samples increased, the thermal breakdown was the dominant factor in the breakdown test. The AC breakdown field strength of all composites tended to decrease, and the reduction of micro-ZnO/LDPE was lower than that of nano-ZnO/LDPE. Besides, the dispersion of the breakdown became better. Moreover, the micro- and nano-ZnO particle doping could improve the conductivity characteristic of polymer effectively. The dielectric constant and dielectric loss of composites increased with the increase of the particle size.

## 1. Introduction

With the growing electricity demand in the world, electricity consumption is increasing year by year. EHV and UHV power transmission has been widely used in the field of power systems. In order to ensure the reliable operation of the power system, researchers focused on how to improve the electrical insulation characteristics. The working life of electric power equipment and the reliable operation of the power system were largely determined by insulation strength. As polyethylene had excellent electrical properties, mechanical properties, and processing properties, it was widely applied to the insulation of high-voltage cables [1, 2]. Polyethylene insulation would be partially discharged under high electric stress for a long time. The electric trees were initiated and spread easily. The space charge accumulation under high

DC voltage would reduce the cable service life and affect the stable operation of the power system. Therefore, the dielectric property improvement of polythene was the key problem. The emergence of nanoparticles provided a new idea for further research. Being compared with polymer/inorganic microcomposites, the polymer/inorganic nanocomposites have some advantages such as high dielectric strength, good performance of partial discharge, and strong electric tree resistance ability [3–8]. But the thermal conductivity and heat blocking effect of microcomposites were better, and the electrical corrosion resistance was excellent [9–12]. According to the synergistic effect of nanocomposites and microcomposites, the dielectric composites could be used in more applications. In this paper, the polyethylene matrix was doped with nano- and micro-ZnO particles, from which the dispersion of particle doping in the matrix could be

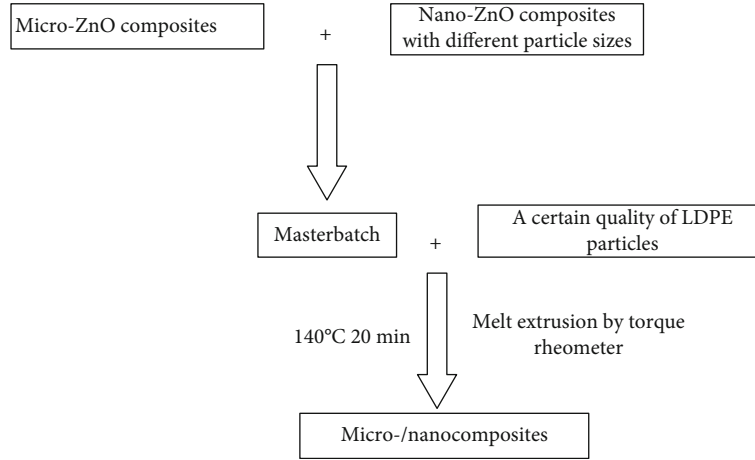


FIGURE 1: Preparation of micro- and nanocomposites with different particle sizes.

explored. Besides, the crystalline properties of different composites could be studied. According to the macroscopic and microcosmic tests, the influence mechanism of inorganic micro- and nanoparticle doping on dielectric properties of composites could be explored. It provided a sufficient theoretical basis for the improvement of polyethylene dielectric properties.

## 2. Preparation and Characterization of Composite

**2.1. Composite Preparation.** In the composite preparation, the low density polyethylene (Daqing Petrochemical) of which density distribution was  $0.910\sim 0.925\text{ mg/cm}^3$  was used as the matrix. The nano-ZnO (DK Nano) of each particle size was 30 nm and  $1\ \mu\text{m}$ . The composites were prepared through melt blending with a torque rheometer, of which the torque was 40 rpm. Among them, the two-step method was used for micro-/nanocomposite preparation. Firstly, a percentage of nano- and micro-ZnO was mixed with LDPE through melt blending. This mixture was used as the masterbatch. Then, the masterbatch was mixed with LDPE, in which the micro-/nanocomposites were prepared [13]. The preparation process of ZnO/LDPE composites is shown in Figure 1. The test sample numbers are shown in Table 1.

**2.2. Morphology Characterization of ZnO.** In order to study the effect of ZnO particle size on LDPE performance, the particle size of the additive was characterized by scanning electron microscope (SEM) before composite preparation, which ensured the accuracy of the particle size. In this process, a small amount of ZnO powder, of which the particle size was 30 nm and  $1\ \mu\text{m}$ , was applied to the conductive adhesive. Then, these samples were observed by SEM, and the observation results are shown in Figure 2.

From Figure 2, the ZnO particle size was 30 nm and  $1\ \mu\text{m}$ . When the particle size was 30 nm, the size distribution was narrower and each particle size was basically the same. While the particle size was  $1\ \mu\text{m}$ , the particle size was mostly accurate but there were some nanoscale-size particles. Besides,

TABLE 1: Different samples and their numbers.

Samples	Content of LDPE (wt%)	Content of ZnO (wt%)	
		30 nm	$1\ \mu\text{m}$
LDPE	100	0	0
30 nm	98	2	0
$1\ \mu\text{m}$	98	0	2
30 nm & $1\ \mu\text{m}$	98	1	1

the particles shape was irregular and the proportion of near-spherical particles was relatively small.

In order to observe the dispersion of ZnO particles in LDPE, SEM was used to observe the composites. Firstly, these samples were processed by low-temperature brittle fracturing in liquid nitrogen. Then, the fracture surfaces were treated by gold spray, and the SEM was used to observe them. The test results are shown in Figure 3.

The SEM of all tested samples are shown in Figure 3. From there, the ZnO particles were dispersed in the matrix uniformly. While the ZnO particle size was  $1\ \mu\text{m}$ , there were some holes in ZnO/LDPE composites, which was shown in the SEM images of m-ZnO with arrowed lines. The reason was that the bonding performance of microparticles with the matrix was too weak. After the brittle fracture, the micro-ZnO particles in the fracture surfaces fell off and the holes existed.

**2.3. Crystalline Properties of Composites.** The DSC was used to observe the crystallization process and crystallinity of ZnO/LDPE composites. Besides, all relevant crystal parameters were tested. The specific steps were as follows. Firstly, these samples were placed in a nitrogen environment, of which the flow was  $150\text{ mL/min}$ . In order to eliminate the thermal history of these samples, they were warmed up to  $140^\circ\text{C}$  at the rate of  $10^\circ\text{C/min}$ , then the temperature dropped down to  $25^\circ\text{C}$ . Secondly, these samples were warmed up to  $140^\circ\text{C}$  again. The enthalpy change of composites during the heating process was recorded. According to automatic

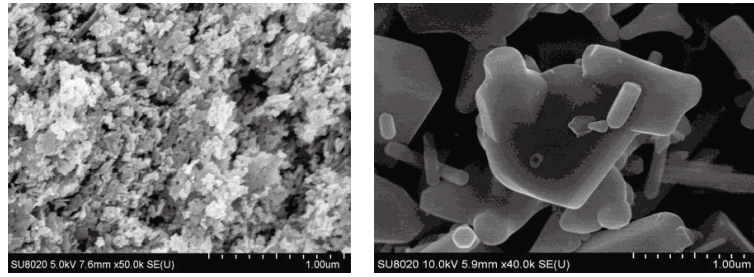


FIGURE 2: Morphology characterization of ZnO with different particle sizes.

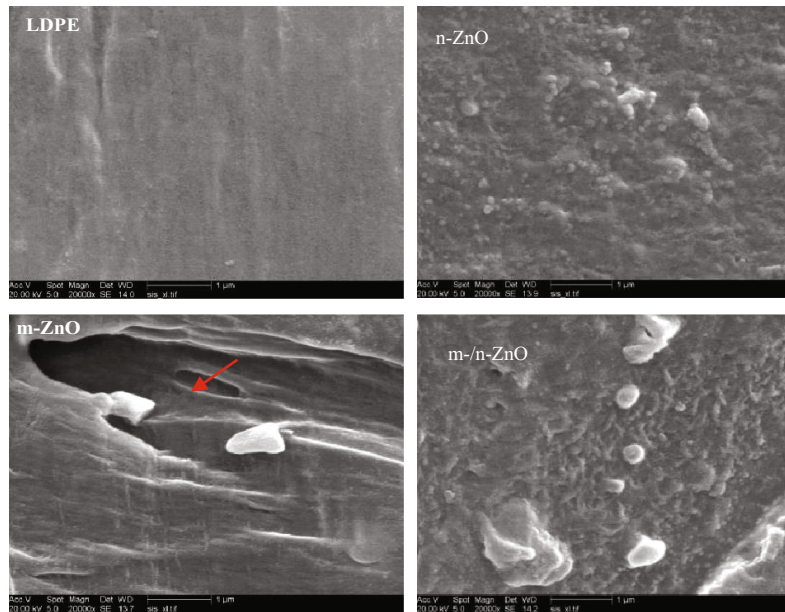


FIGURE 3: Micro characterization of composite materials.

analysis, the melting peak temperature  $T_m$  and the melting heat  $\Delta H_m$  could be calculated [14, 15]. The DSC test results of different materials are shown in Figure 4.

According to the parameters above and formula (1), the crystallinity of LDPE and various ZnO/LDPE composites could be calculated:

$$X_c = \frac{\Delta H_m}{(1 - \omega)H_0} \times 100\%. \quad (1)$$

In formula (1),  $\Delta H_m$  was the melting heat of materials (J/g).  $H_0$  was the melting heat of composites under holocrystalline, which was 293.6 J/g for LDPE.  $\omega$  was the mass fraction of ZnO with different particle sizes [16].

The composite parameters tested by DSC in isothermal crystallization and the melting process are shown in Table 2.

From Table 2, after micro- and nano-ZnO particle doping, the melting peak temperatures of micro- and nanocomposites were the same with LDPE. Among them, the melting peak temperature of microcomposites was slightly higher. Besides, the exothermic crystallization peak width  $\Delta T_c$  of micro- and nanocomposites was lower than that of pure LDPE. Because the width of  $\Delta T_c$  represented the crystalliza-

tion rate of composites, the micro- and nano-ZnO doping improved the crystallization rate of polymer effectively. The crystallinity of all composites was improved, but the degree was different. The crystallinity order of different samples was as follows: 30 nm > 30 nm/1  $\mu$ m > 1  $\mu$ m > LDPE. The crystallinity of the micro-/nanocomposites was a medium between microcomposites and nanocomposites.

### 3. Results and Analysis of Macroscopic Experiment

**3.1. Breakdown Characteristics of Micro- and Nano-ZnO/LDPE Composites.** The breakdown strength of dielectric materials was affected by many factors including the internal and environmental factors, such as electrode materials, space charge distribution, temperature, and chemistry. It was a complex procedure, which was restricted by multiple factors. Therefore, the experimental data of breakdown was processed by Weibull distribution based on the weak electricity breakdown theory.

The different samples were tested by the DC breakdown system and the AC breakdown system, and the

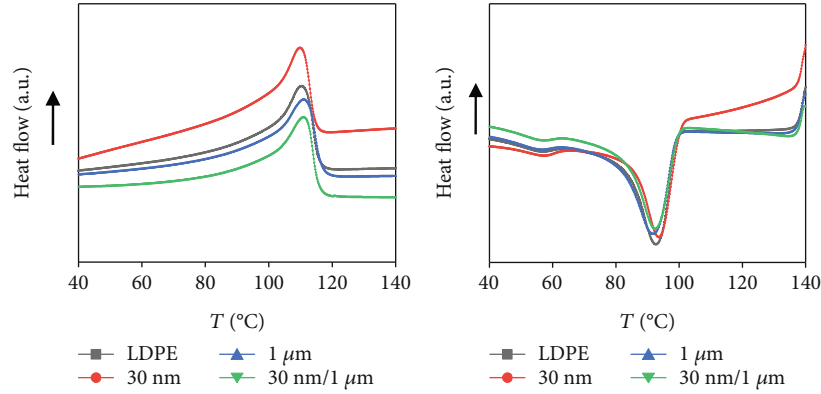


FIGURE 4: DSC test curve of composite materials.

TABLE 2: Different samples and their numbers.

Sample	Crystalline peak temperature, $T_c$ (°C)	Melting temperature, $T_m$ (°C)	Width of exothermic crystalline peak, $\Delta T_c$ (°C)	Crystallinity, $X_c$ (%)
LDPE	93.24	109.78	8.54	34.26
30 nm	94.12	109.24	6.22	39.77
1 $\mu\text{m}$	92.36	110.51	6.02	35.45
30 nm & 1 $\mu\text{m}$	93.79	109.94	6.90	37.55

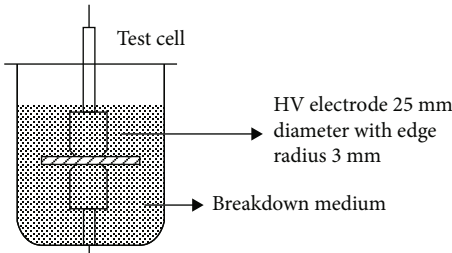


FIGURE 5: Electrode configuration in AC/DC breakdown experiments.

electrode configuration in AC/DC breakdown experiments is shown in Figure 5.

Under the AC electric field, the breakdown strength of composites with different thicknesses was tested, from which the effect of thickness on breakdown strength could be found. In the course of this experiment, a whole set of experimental systems were placed into the cable oil, which prevents the samples from surface discharge. This system boosted at a speed of 1 kV/s until the material breakdown, and the breakdown field strength was recorded. Each sample was tested for 20 points. According to the formula  $E = U/d$ , the breakdown field strength of micro- and nano-ZnO/LDPE composites could be calculated. The Weibull distribution was used for data processing.

**3.1.1. AC Breakdown Characteristics.** The thickness of samples was  $65 \pm 10 \mu\text{m}$ ,  $130 \pm 10 \mu\text{m}$ , and  $195 \pm 10 \mu\text{m}$ . The Weibull distribution of the AC breakdown test in different materials is shown in Figures 6–8. The shape parameters ( $\beta$ ) and Weibull breakdown field strength ( $E_0$ ) are shown in Tables 3–5.

Combining the result of Figure 6 and Table 3, when the thickness of samples was  $65 \pm 10 \text{ nm}$ , the breakdown field strength of nano-ZnO/LDPE and micro-/nano-ZnO/LDPE was higher than that of pure LDPE. When the ZnO particle size was 30 nm, the breakdown field strength of composites was the highest at 138.0 kV/mm, which increased by 8.24% compared to pure LDPE. The breakdown field strength of micro-ZnO/LDPE was lower than that of LDPE, which was 113.4 kV/mm and decreased by 11.1% compared to pure LDPE. The breakdown field strength of the micro-/nanocomposite was a medium between microcomposite and nanocomposite, and the breakdown field strength of LDPE was the lowest.

Combining the result of Figure 7 and Table 4, when the thickness of samples was  $130 \pm 10 \mu\text{m}$ , the variation of breakdown field strength with ZnO particle size was similar to the samples with  $60 \pm 10 \mu\text{m}$  thickness. When the ZnO particle size was 30 nm, the breakdown field strength was the highest at 122.7 kV/mm, which increased by 8.3% compared to pure LDPE. When the ZnO particle size was 1  $\mu\text{m}$ , the breakdown field strength of micro-ZnO/LDPE was 9.2% lower than that of pure LDPE, and the breakdown field strength of micro-/nanocomposites was slightly higher than that of pure LDPE.

Combining the result of Figure 8 and Table 5, when the thickness of samples was  $195 \pm 10 \mu\text{m}$  and the ZnO particle size was 30 nm, the breakdown field strength of nano-ZnO/LDPE was 1.7% higher than that of pure LDPE. It was 86.06 kV/mm. When the ZnO particle size was 1  $\mu\text{m}$ , the breakdown field strength of micro-ZnO/LDPE was the lowest at 78.34 kV/mm, which decreased by 8.9% compared to pure LDPE. The breakdown field strength of micro-/nano-ZnO/LDPE was lower than that of pure LDPE.

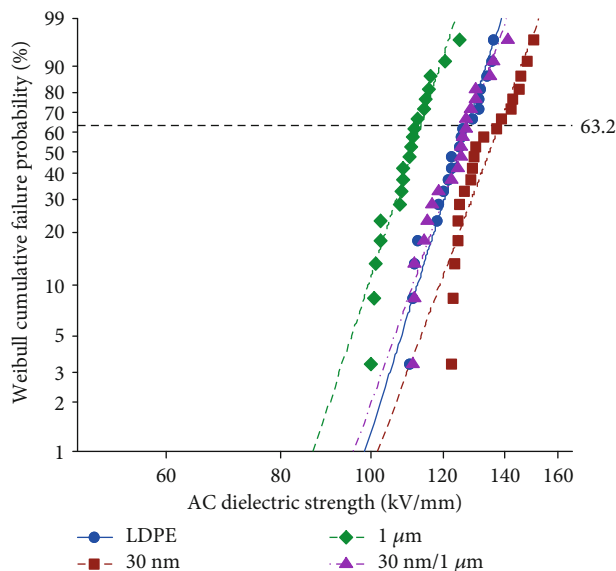


FIGURE 6: AC breakdown field strength of different particle sizes and micro-/nanocomposite materials with a thickness of  $65 \pm 10 \mu\text{m}$ .

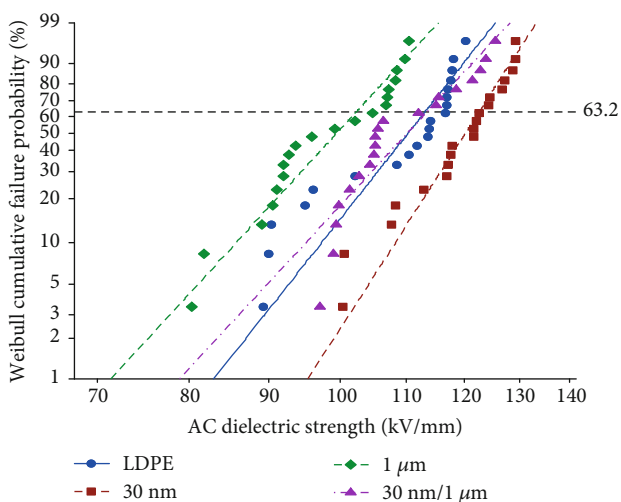


FIGURE 7: AC breakdown field strength of different particle sizes and micro-/nanocomposite materials with a thickness of  $130 \pm 10 \mu\text{m}$ .

In order to explore the effect of inorganic particle doping on breakdown characteristics of the polymer, the models of the inner electron transportation path in micro- and nano-ZnO composites were built, which are shown in Figure 9.

From Figure 9, the conductive path of composite was more circuitous due to the nanoparticle doping, and it could improve the breakdown characteristics of the composite more efficiently than microparticle doping. Therefore, the breakdown field strength of nano-ZnO/LDPE was the highest. And since the nano-ZnO particle doping played a role in heterogeneous nucleation agent, the crystallinity and interfacial structure of composites increased. There were lots of traps in the interface region. In the process of movement to the electrode, the internal carriers were trapped easily. This would cause a decrease of free volume. Besides, the free path

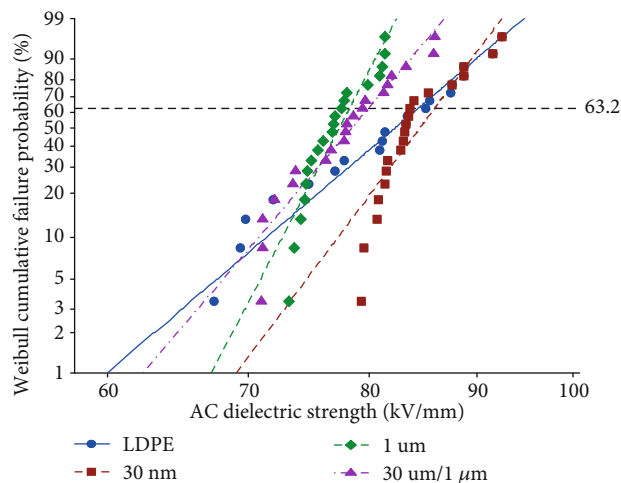


FIGURE 8: AC breakdown field strength of different particle sizes and micro-/nanocomposite materials with a thickness of  $195 \pm 10 \mu\text{m}$ .

TABLE 3: AC breakdown characteristics of different particle sizes and micro-/nanocomposite materials with a thickness of  $65 \pm 10 \mu\text{m}$ .

Samples	Breakdown field strength, $E_b$ (kV/mm)	Number (N)	Shape parameters ( $\beta$ )
LDPE	127.5	20	17.96
30 nm	138.0	20	15.15
1 $\mu\text{m}$	113.4	20	17.21
30 nm & 1 $\mu\text{m}$	128.0	20	15.96

TABLE 4: AC breakdown characteristics of different particle sizes and micro-/nanocomposite materials with a thickness of  $130 \pm 10 \mu\text{m}$ .

Samples	Breakdown field strength, $E_b$ (kV/mm)	Number (N)	Shape parameters ( $\beta$ )
LDPE	113.3	20	14.79
30 nm	122.7	20	18.27
1 $\mu\text{m}$	102.4	20	12.72
30 nm & 1 $\mu\text{m}$	113.7	20	12.61

TABLE 5: AC breakdown characteristics of different particle sizes and micro-/nanocomposite materials with a thickness of  $195 \pm 10 \mu\text{m}$ .

Samples	Breakdown field strength, $E_b$ (kV/mm)	Number (N)	Shape parameters ( $\beta$ )
LDPE	84.58	20	13.35
30 nm	86.06	20	20.98
1 $\mu\text{m}$	78.34	20	30.14
30 nm & 1 $\mu\text{m}$	80.06	20	18.47

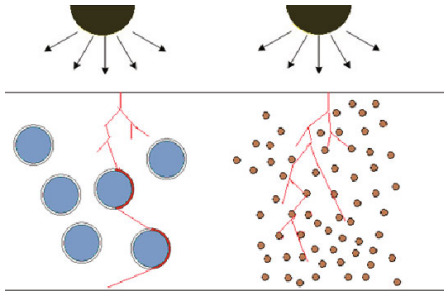


FIGURE 9: Inner electron transportation path of different ZnO composites. Large circles: micro fillers; small circles: nanofillers; half ball: needle electrode.

was longer, and the electrons had difficulty in obtaining enough kinetic energy. The binding abilities between micro-particles and the polymer were poor. The interfacial structure was loose and the trapping effect was weak. Combining the SEM result of microparticles, there were parts of irregular particles in the micro-ZnO, of which shapes were rod-like and regular tetrahedron. Besides, the defect effect was introduced by microparticles, so the breakdown field strength of microcomposites was the lowest. The breakdown field strength of micro-/nanocomposites was a medium between microcomposites and nanocomposites. With the increase of thickness, the breakdown field strength in different materials decreased. It was found that the thicker the sample thickness, the lower the breakdown field strength [17–19]. When the AC voltage was applied to composites, electric breakdown and thermal breakdown would happen. When the thickness was thinner, the electric breakdown played a leading role in breakdown field strength, and the breakdown strength of composites was related to the interface regional characteristic. With the sample thickness increased, the heat generated by composite loss under the electric field could not escape effectively. The heat accumulation was very serious, and the breakdown strength of composites was greatly affected by thermal breakdown. It found that the thicker the sample thickness, the harder the heat dissipation. The influential role of thermal breakdown was more obvious, and the breakdown field strength decreased even more. On the other hand, the breakdown of composites was one kind of weak point breakdown. With the sample thickness increased, the samples became larger, and the weak points would increase. It also reduced the breakdown field strength of composites. The reduction degree of the breakdown field strength of microcomposites was lower than that of nanocomposites. The reasons were chiefly as follows: the solid thermal conducting mechanism was closely related to microscopic particle movement. In the process of heat transfer, the propagation media were phonons, photons, and electrons mainly. For ZnO/LDPE composites, the electrons were the major heat propagation medium. The thermal conductivity of composite depended on the quantity of free electrons [20, 21]. The larger the quantity of free electrons, the better the thermal conductivity. According to the above, the traps generated by ZnO/LDPE composites would capture the electrons. The quantity of free electrons decreased and the thermal resistance per unit volume of material was high, so the

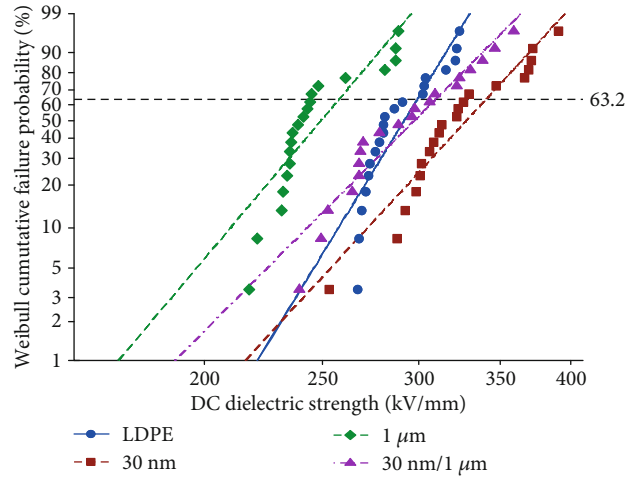


FIGURE 10: DC breakdown field strength of different particle sizes and micro-/nanocomposites.

TABLE 6: DC breakdown characteristics of different particle sizes and micro-/nanocomposites.

Samples	Breakdown field strength, $E_b$ (kV/mm)	Number (N)	Shape parameters ( $\beta$ )
LDPE	299.0	20	15.25
30 nm	340.4	20	10.14
1 $\mu\text{m}$	257.8	20	11.06
30 nm & 1 $\mu\text{m}$	309.3	20	9.366

thermal conductivity was poor. The interface region introduced by the microcomposite was smaller, which had a little effect on the trap level and density. The quantity of free electrons increased, so the thermal conductivity of microcomposites was better than that of nanocomposites. With the sample thickness increased, the reduction degree of the breakdown field strength of microcomposites was lower than that of nanocomposites.

**3.1.2. DC Breakdown Characteristics.** Under the DC electric field, the breakdown characteristic experiment was implemented on pure LDPE and different kinds of ZnO/LDPE composites. The sample thickness was  $65 \pm 10 \mu\text{m}$ . The breakdown electrode in this experiment was the same with that in the AC breakdown experiment. The Weibull distribution of the DC breakdown test in different samples is shown in Figure 10. The shape parameters  $\beta$  and breakdown field strength  $E_0$  under Weibull distribution are shown in Table 6.

Combining the result of Figure 10 and Table 6, the DC breakdown field strength was higher than the AC breakdown field strength in pure LDPE and different kinds of ZnO/LDPE composites. The breakdown field strength order of different samples was as follows:  $30 \text{ nm} > 30 \text{ nm}/1 \mu\text{m} > 1 \mu\text{m} > \text{LDPE}$ . Among them, the DC breakdown field strength of nanocomposites was the highest, the microcomposite was the lowest, and the micro-/nanocomposite was a medium

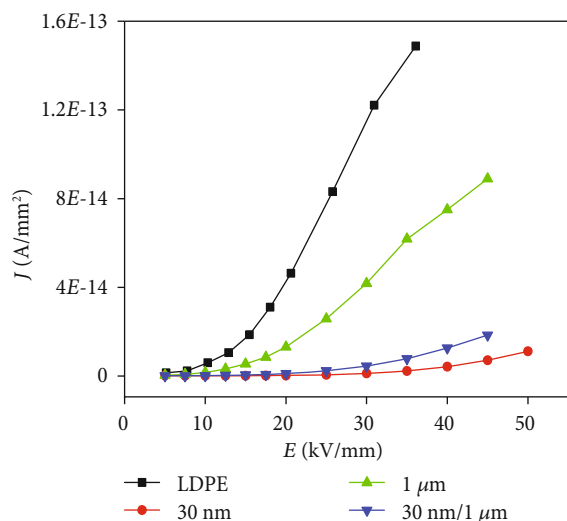


FIGURE 11: Conductivity curves of different particle size ZnO/LDPE composites.

between the microcomposite and the nanocomposite. The reason was that the AC breakdown proceeded under an AC electric field and the carriers move back and forth across the two electrodes. While under the DC electric field, the carriers only moved to the positive electrode. The impact ionization seldom appeared, so the DC breakdown field strength was higher than the AC breakdown field strength [22]. The change rule of the DC breakdown field strength in different samples was the same with that of the AC breakdown field strength. Lots of traps were introduced due to the smaller size of nanoparticles. It restricted the carrier migration and enhanced the breakdown field strength. When the particle size increased, the interface of composites would decrease, which weakened the trap effect. When the particles size was  $1 \mu\text{m}$ , it served as the impurity particles introduced to LDPE, which reduced the breakdown field strength most.

**3.2. Conductivity Characteristic.** The HV DC power was used in this experiment. The conductivity characteristics of these samples were tested by picoammeters. Combined with the microstructure, the charge injection and transport of composites were explored further, which applied the theoretical basis for the development of higher performance insulating material.

**3.2.1. The Effect of Electric Field on Conductivity Characteristic.** From the data-analyzing results, the relationship curve of different electric fields and current densities could be obtained. The relationship curve of the electric field and current density in different samples is shown in Figure 11.

From Figure 11, the current density of different samples had an exponent relation with electric field strength, but with different sizes. Under the same field strength, the current density order of different samples was as follows:  $30 \text{ nm} > 30 \text{ nm}/1 \mu\text{m} > \text{LDPE}$ .

The reason was that the steady-state conduction current was formed by carrier movement. For pure LDPE, the carriers were mainly composed of electrons and ions. Under

applied voltage, the electron would be injected from the electrode to samples. Therefore, as the electric field strength increased, the electric force which the dielectric electrons and ions suffered by was increased. On the other hand, the dielectric electrons which were injected from the electrode increased. It caused the accretion of carrier concentration and mobility. According to formula (1), the current density of pure LDPE increased [23]. After ZnO particle doping, the heterogeneous nucleation of ZnO formed the interphase of additive and pure LDPE, from which the traps were introduced and the carrier was trapped. The carrier concentration and mobility decreased. Therefore, the current density of composites was lower than that of pure LDPE. The nanoparticle doping could lead to the deep traps. With the increase of trap density, the nanoeffect was significant. Among them, the current density of nanocomposites was the least.

**3.2.2. The Effect of Temperature on Electrical Conductivity of Composite.** According to the analysis of carrier concentration and mobility in thermal equilibrium, the effect of temperature on electrical conductivity could be explored. With the increase of temperature, the energy of the carrier increased. According to the energy band theory, the charges obtained more energy with a sufficiently high temperature, which made them cross the forbidden band to the conduction band. The electrical conductivity would increase as well. Besides, various conductance forms coexisted dielectrically, and the temperature had a more obvious effect on the electrical conductivity of composites. Under the  $20 \text{ kV/mm}$  field strength, the current density of composites in  $25^\circ\text{C}$ ,  $45^\circ\text{C}$ ,  $60^\circ\text{C}$ ,  $75^\circ\text{C}$ , and  $90^\circ\text{C}$  was measured. Besides, according to the space charge limited current effect above, the charge trapping and detrapping would happen in test samples under a high electric field [24]. These charges would affect the measurement results. In order to reduce this error, after the conductance measurement in one temperature point, the samples must be placed in an oven for 2 h. Then, the conductance measurement of the next temperature point can proceed. The test results of temperature on current density in different samples are shown in Figure 12.

From Figure 12, within the test range of the whole experimental temperature, the current density of different samples increased with the temperature raised. While the temperature was low, the conductivity changed a little. At this time, the current density of samples was less dependent on temperature. Under the same temperature, the current density of the nanocomposite and micro-/nanocomposite was lower, and the microcomposite was higher. But all of them were lower than those of pure LDPE.

The test results of temperature on electrical conductivity in different samples are shown in Figure 13. The electrical conductivity in different samples increased with the temperature increase, and the degree of increase was basically consistent. But the electrical conductivity in all composites was lower than that of LDPE. It also proved that the thermal excitation hopping process existed in the conductive mechanism of composites. The reason was due to the temperature rise; the dielectric carrier took more power and overcame the barrier between energy bands. The carrier concentration and

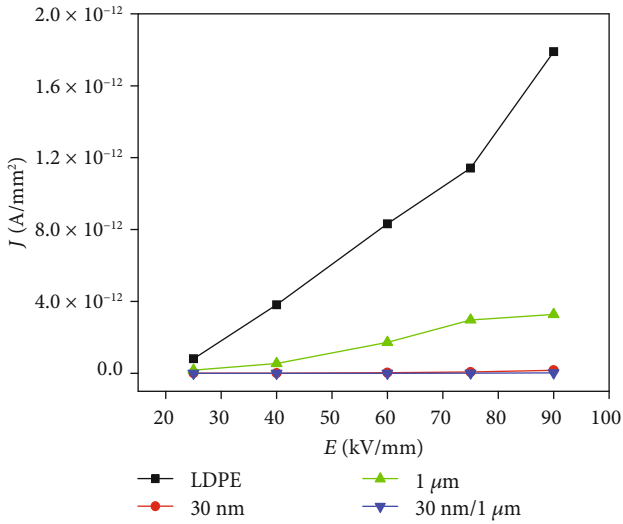


FIGURE 12: Current density of different particle size ZnO/LDPE composites with temperature variation curve.

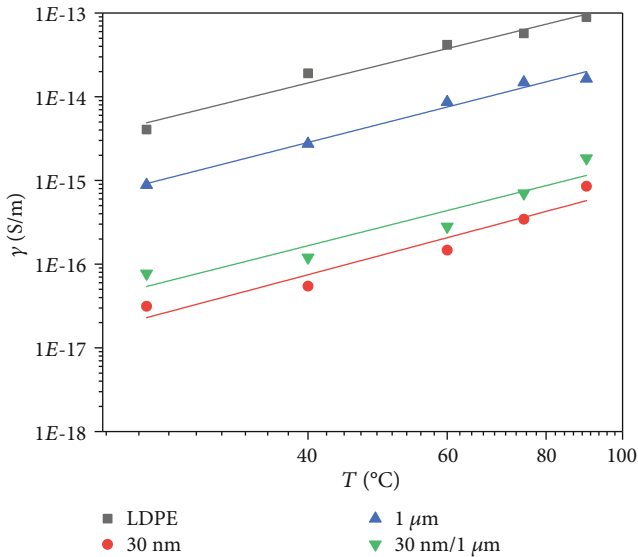


FIGURE 13: Electrical conductivity of different particle size ZnO/LDPE composites with temperature variation curve.

current density increased. On the other hand, when the temperature was constant, the temperature mainly affected the dielectric ionic conductance. The ionic conductance could be divided into intrinsic ionic conductance and weakly bound impurity ion conductance. At low temperature, the dielectric conductance was formed by weakly bound impurity ions. While at high temperature, the polymer disassociation would lead to the emergence of intrinsic ionic conductance. The carrier concentration increased further, and the varying degrees of current density with temperature were greater [25]. But with micro-ZnO particle doping, the shallow traps would be introduced into the matrix. The intermolecular force between microparticles and the polythene matrix was weak. With the rise of temperature, the carrier was easy to migrate. Therefore, the conductivity of micro-

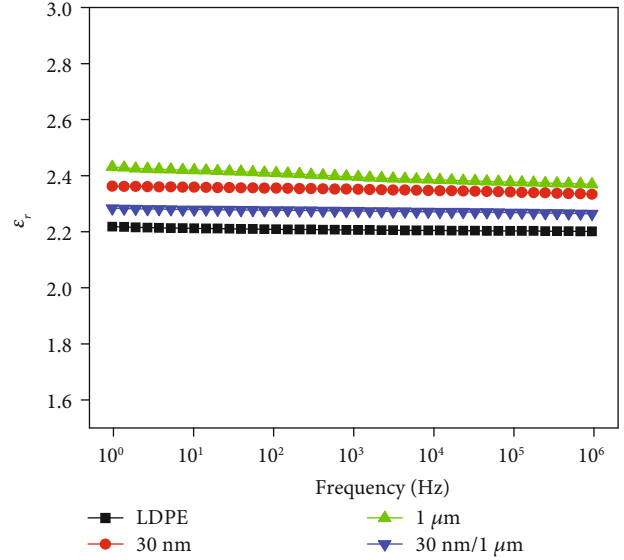


FIGURE 14: Frequency dependence of relative permittivity of micro-/nano-ZnO/LDPE composites.

ZnO/LDPE composites was more affected by temperature, while the nanoparticle doping and micro-/nanoparticle doping would introduce the deep traps into the polythene matrix, which restrained the carrier migration effectively. Therefore, the conductivity of nanocomposites and micro-/nanocomposites was less affected by temperature.

**3.3. Dielectric Frequency Spectrum Test.** The polarization is a special dielectric phenomenon under an electrical field, which is caused by material interior positive and negative electric charge center separation. Dielectric loss was caused by conductance and polarization under an applied electric field. The relative dielectric constant and dielectric loss angular tangent value were expressed by  $\epsilon_r$  and  $\tan \delta$ . The relationship curve of  $\epsilon_r$ ,  $\tan \delta$ , and frequency was described as the dielectric frequency spectrum. LDPE was nonpolar dielectric, of which the main polarization type was displacement polarization under an electric field. After nano- and micro-ZnO particle doping, the new polarization type would be introduced into the composites. A large number of interfaces were formed between the additive and the matrix, and a massive interfacial polarization existed [26].

**3.3.1. The Effect of Frequency on Dielectric Constant.** In this experiment, the relationship curve of the dielectric constant and frequency of LDPE and ZnO/LDPE composites was measured by a dielectric frequency spectrum analyzer (Alpha-A, Novocontrol Technologies, Germany). The test range of experimental frequency was 1 Hz to 10<sup>6</sup> MHz. Before testing, the samples must be treated by short circuit in the oven for 12 h. The relationship curve of the dielectric constant and frequency of different samples is shown in Figure 14.

From Figure 14, in the whole frequency, the variation trend of the dielectric constant in ZnO/LDPE composites and LDPE was the same. In comparison, the dielectric constant of composites was higher. When the particles size was 1 μm, the dielectric constant of the ZnO/LDPE composite

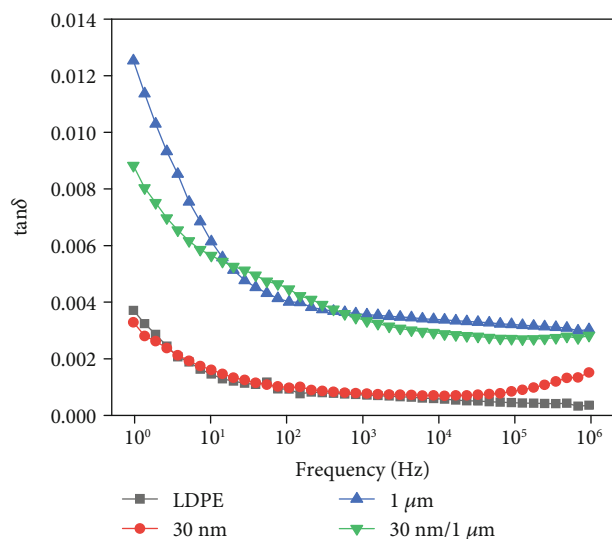


FIGURE 15: Frequency dependence of dissipation factor of micro-/nano-ZnO/LDPE composites.

was the highest. Besides, in the whole testing frequency, the dielectric constant of most samples was basically unchanged. But the microcomposite was an exception. When the frequency increased, the dielectric constant decreased gradually.

The reasons were chiefly as follows: the pure LDPE was one kind of nonpolar dielectric, in which the polarization type was electronic displacement polarization. These polarizations had little change with the variation of electric field frequency. As an additive, the content of ZnO was less, so the dielectric constant of ZnO/LDPE composites was similar to that of pure LDPE. But ZnO was one kind of polar material. With the ZnO particles being doped into LDPE, a new polarization type would be introduced, such as ionic displacement polarization and interfacial polarization, which would cause the increase of the dielectric constant. When the particles size was  $1\ \mu\text{m}$ , the binding effect of microparticles on polymer chains would be weakened. Besides, the dielectric constant of ZnO was higher, which would cause the Maxwell-Wagner interfacial polarization in composites. So the dielectric constant of the microcomposite was higher than that of pure LDPE. On the other hand, this interfacial polarization was one kind of relaxation polarization. The polarization time was longer, and the polarization process would be affected by frequency. When the testing frequency increased to high frequency, the relaxation polarization was hard to complete. Therefore, the relative dielectric constant of the microcomposite decreased gradually.

**3.3.2. The Effect of Frequency on Loss Angle Tangent Value.** The change curve of the loss angle tangent value and frequency in different samples is shown in Figure 15.

From Figure 15, in the whole frequency, the loss angle tangent value of different samples first decreased then evolved toward a steady-going value with the increase in frequency. The loss angle tangent value of the microcomposite and micro-/nanocomposite was higher than that of pure LDPE, and the loss angle tangent value of the nanocomposite

was basically the same with that of pure LDPE. The reasons were chiefly as follows: after an additive was doped into the polymer, the interface between particles and the matrix formed. Under applied electrical field, the dipole moment would be formed by interfacial polarization, which improved the loss factor of the composite. Among them,  $\tan\ \delta$  of the microcomposite was the highest. The polarity effect of ZnO led to a rise in  $\tan\ \delta$ . With the frequency increasing to a high frequency, the interfacial polarization could not keep up with the changing frequency of the applied electric field, and the polarization was hard to complete. Therefore, the  $\tan\ \delta$  of LDPE and different composites would decrease gradually, then evolved toward a steady-going value.

## 4. Conclusions

In this article, pure LDPE was used as matrix materials and micro- and nano-ZnO particles were used as inorganic filler. According to the two-step melt blending, the micro- and nanocomposites were prepared. SEM and DSC experiments were used to characterize the surface morphology and crystallization of different samples. Besides the breakdown properties, DC conductivity properties and dielectric properties of LDPE and different composites were tested, from which the conclusions were drawn as follows:

- (1) According to the result of SEM, when the particles size was 30 nm, each particles size of ZnO was basically uniform, and the morphology was globe-like. There were some nanoscale particles in micro-ZnO, but the morphology of most particles was irregular. From the SEM result of ZnO/LDPE composites, the ZnO particles were dispersed well in LDPE, and the powder particle size remained unchanged before and after composite
- (2) According to the result of DSC, ZnO particles being doped into LDPE played the role of heterogeneous nucleation agent. The crystallization rate of the composites increased. The crystallinity of composites was higher than that of pure LDPE. The fraction of crystalline areas increased and the amorphous areas was circuitous. Among them, the crystallinity of nano-ZnO/LDPE was the highest, which was 16.1% higher than pure LDPE
- (3) According to the result of the AC and DC breakdown characteristic test, the breakdown field strength of nano-ZnO/LDPE was the highest and the breakdown field strength of the micro-/nanocomposite was a medium between the microcomposite and the nanocomposite. This experimental result was consistent with DSC. During the AC breakdown characteristic test, the thermal breakdown played a leading role with the increase of sample thickness, which caused the breakdown field strength degradation obviously. Among them, the breakdown field strength decreasing degree of micro-ZnO/LDPE was lower than that of nano-ZnO/LDPE, and the thermal breakdown properties of micro-ZnO/LDPE were better

- (4) According to the result of conductivity properties, with the micro- and nano-ZnO particles being doped into LDPE, the effect of interface traps was obvious, and the carrier mobility decreased. The current density of all composites was less than that of pure LDPE, and the current density of the micro-/nanocomposite was a medium between the microcomposite and the nanocomposite. At different temperatures, the current density of LDPE and composites increased linearly with the rise of temperature, and the current density of LDPE was the highest
- (5) Nano-ZnO particles were one kind of polar material. According to the result of the dielectric frequency spectrum test, with the nano-ZnO particles being doped into LDPE, a new polarization type was introduced. The dielectric constant of nano-ZnO/LDPE was higher than that of pure LDPE. Besides, the dielectric loss of all composites was higher than that of pure LDPE

### Data Availability

All data generated or analyzed during this study are included in this article.

### Conflicts of Interest

The authors declare no conflicts of interest.

### Authors' Contributions

Conceptualization of this article was done by Yu Guang, methodology by Cheng Yujia and Yu Guang, formal analysis by Yu Guang and Duan Zhuohua, and investigation by Cheng Yujia; resources were provided by Duan Zhuohua and data curation by Cheng Yujia and Yu Guang; and writing (original draft preparation) was handled by Cheng Yujia, writing (review and editing) by Yu Guang, supervision by Duan Zhuohua, project administration by Cheng Yujia, and funding acquisition by Duan Zhuohua.

### Acknowledgments

This research was aided by the Science and Technology Planning Program of Zhongshan City, China, under grant no. 2018B1018. The authors thank professor Duan Zhuohua and Doctor Yu Guang for their help.

### Supplementary Materials

The description of editable figure files 4: AC breakdown field strength of different particle sizes and micro-/nanocomposite materials with a thickness of  $195 \pm 10 \mu\text{m}$ . (*Supplementary Materials*)

### References

- [1] X.-x. Zhou, Z.-x. Lu, Y.-m. Liu, and S.-y. Chen, "Development models and key technologies of future grid in China," *Proceedings of the CSEE*, vol. 34, no. 29, pp. 4999–5008, 2014.
- [2] D.-h. Zhang, H. Zhang, Z. Zhang, and Y.-f. Chen, "The application of nanotechnology in high performance electric power composite insulation materials," *Science China Press*, vol. 43, no. 6, pp. 725–743, 2013.
- [3] J.-l. Guo, C. Yu, and Z.-r. Jia, "Study on electrical properties of micro-nano structured epoxy composites," in *Proceedings of 2014 International Symposium on Electrical Insulating Materials*, pp. 441–444, Niigata, Japan, June 2014.
- [4] S. Alapati, J. T. Meledath, and A. Karmarkar, "Effect of morphology on electrical treeing in low density polyethylene nanocomposites," *IET Science, Measurement & Technology*, vol. 8, no. 2, pp. 60–68, 2014.
- [5] M. H. Ahmad, N. Bashir, H. Ahmad, A. Jamil, and A. A. Suleiman, "An overview of electrical tree growth in solid insulating material with emphasis of influencing factors, mathematical models and tree suppression," *TELKOMNIKA Indonesian Journal of Electrical Engineering*, vol. 12, no. 8, pp. 5827–5846, 2014.
- [6] J.-W. Zha, Y.-H. Zhu, and W.-K. Li, "Low dielectric permittivity and high thermal conductivity silicone rubber composites with micro-nano-sized particles," *Applied Physics Letters*, vol. 101, no. 6, article 062905, 2012.
- [7] J.-m. Yang, X. Wang, H. Zhao, W.-l. Zhang, and X. Mingzhong, "Influence of moisture absorption on the DC conduction and space charge property of MgO/LDPE nanocomposite," *IEEE Transactions on Dielectrics and Electrical Insulation*, vol. 21, no. 4, pp. 1957–1964, 2014.
- [8] F. Yu, W. L. Li, Y.-f. Hou et al., "Enhanced dielectric properties of PVDF-HFP/BaTiO<sub>3</sub>-nanowire composites induced by interfacial polarization and wire-shape," *Journal of Materials Chemistry C*, vol. 3, no. 6, pp. 1250–1260, 2015.
- [9] E. Tuncer and I. Sauers, "Industrial applications perspective of nanodielectrics," in *Dielectric Polymer Nanocomposites*, J. Nelson, Ed., pp. 321–338, Springer, Boston, MA, 2010.
- [10] D. Fabiani and G. C. Montanari, "Epoxy based materials containing micro and nano sized fillers for improved electrical characteristics," in *2010 10th IEEE International Conference on Solid Dielectrics*, pp. 1–4, Germany, Potsdam, July 2010.
- [11] Y. Hayase, Y. Tanaka, and T. Takada, "Space charge suppression effect of nano-size fillers added to polymeric materials," *Measurement Analysis and Applications, 40th Anniversary Meeting*, 2009, 1997–2000.
- [12] S.-t. Li, G.-l. Yin, and S.-n. Bai, "A new potential barrier model in epoxy resin nanodielectrics," *Transactions on Dielectrics and Electrical Insulation*, vol. 18, no. 5, pp. 1535–1543, 2011.
- [13] Y.-l. Zhao, *Study on Preparation and Performance of ZnO and Composite*, Zhengzhou University, Zhengzhou, China, 2011.
- [14] C.-s. Zhu, *Structural Analysis of Polymer*, China Science Publishing & Media Ltd, Beijing, 2004.
- [15] Z.-s. Mo, H.-f. Zhang, and J.-d. Zhang, *Crystalline Polymer Structure and X-Ray Diffraction*, China Science Publishing & Media Ltd, Beijing, 2010.
- [16] O. K. Muratoglu, A. S. Argon, and R. E. Cohen, "Toughening mechanism of rubber-modified polyamides," *Polymer*, vol. 36, no. 5, pp. 921–930, 1995.
- [17] Y.-j. Cheng, X.-h. Zhang, and N. Guo, "Effects of nano-ZnO and nano-montmorillonite on dielectric properties of low density polyethylene," *Journal of Composite Materials*, vol. 32, no. 1, pp. 94–100, 2015.
- [18] S. Virtanen, A. S. Vaughan, and L. Yang, *Dielectric Breakdown Strength and Electrical Conductivity of Low Density*

*Polyethylene Octylnanosilica Composite Electrical Insulation and Dielectric Phenomena*, IEEE, Toronto, Canada, 2016.

- [19] D. Ma, T. A. Hugener, and R. W. Siegel, "Influence of nanoparticle surface modification on the electrical behaviour of polyethylene nano-composites," *Nanotechnology*, vol. 16, no. 6, pp. 724–731, 2005.
- [20] M. Meunier, N. Quirke, and A. Aslanides, "Molecular modeling of electron traps in polymer insulators: chemical defects and impurities," *Journal of Chemical Physics*, vol. 115, no. 6, pp. 2876–2881, 2001.
- [21] K. Huang and J. Rzayev, "Charge and size selective molecular transport by amphiphilic organic nanotubes," *Journal of the American Chemical Society*, vol. 133, no. 42, pp. 16726–16729, 2011.
- [22] Y. Jin, N. Xia, and R. A. Gerhardt, *Dielectric nanocomposite with high dielectric permittivity and low dielectric loss*, Electrical Insulation Conference, Seattle, WA, USA, 2015.
- [23] K. Xiao, Y. Wang, and C. Wang, *Study on Space Charge Behaviors and Trap Characteristics in LDPE/SiO<sub>2</sub> under Thermal Aging*, Electrical Insulation and Dielectric Phenomena, Toronto, Canada, 2016.
- [24] F.-q. Tian, Q.-q. Lei, and X. Wang, "Effect of deep trapping states on space charge suppression in polyethylene/ZnO nanocomposite," *Applied Physics Letters*, vol. 99, no. 14, article 142903, 2011.
- [25] X. Cheng, S. Q. Chen, and X. Wang, "In the process of polyethylene electrical aging, the influence of nanometer ZnO for space charge and the breakdown characteristics," *Insulation materials*, vol. 41, no. 1, pp. 44–48, 2008.
- [26] J. Xu and C. P. Wong, "Effects of the low loss polymers on the dielectric behavior of novel aluminum-filled high-K nanocomposites," in *International Symposium on Advanced Packaging Materials: Processes, Properties and Interface*, pp. 158–170, IEEE Dielectrics and Electrical Insulation Society, New York, 2004.



**Hindawi**  
Submit your manuscripts at  
[www.hindawi.com](http://www.hindawi.com)

